MBIP (MAP3K12 binding inhibitory protein) drives NSCLC metastasis by JNK-dependent activation of MMPs

Joshua Kapere Ochieng[1,3], **Samrat T. Kundu**[1,3,#], **Rakhee Bajaj**[1], **B. Leticia Rodriguez**[1], **Jared J. Fradette**[1], **Don L. Gibbons**[1,2,#]

[1]Department of Thoracic/Head and Neck Medical Oncology, The University of Texas MD Anderson Cancer Center, 1515 Holcombe Blvd, Houston, TX, USA

[2]Department of Molecular and Cellular Oncology, University of Texas MD Anderson Cancer Center, 1515 Holcombe Blvd, Houston, TX 77030, USA

[3]Authors contributed equally

Abstract

Metastasis is the cause for 90% of cancer-related mortalities. Identification of genetic drivers promoting dissemination of tumor cells may provide opportunities for novel therapeutic strategies. We previously reported an *in vivo* gain-of-function screen that identified ~30 genes with a functional role in metastasis promotion and characterized detailed mechanistic functions of two hits. In the present study, we characterized the contribution of one of the identified genes, MBIP (MAP3K12 binding inhibitory protein), towards driving tumor invasion and metastasis. We demonstrate that expression of MBIP significantly enhances the cellular proliferation, migration and invasion of NSCLC cells *in vitro* and metastasis *in vivo*. We functionally characterized that MBIP mediates activation of the JNK pathway and induces expression of matrix metalloproteinases (MMPs), which are necessary for the invasive and metastatic phenotype. Our findings establish a novel mechanistic role of MBIP as a driver of NSCLC progression and metastasis.

Introduction

Lung cancer remains the leading cause of cancer-related mortality due to its propensity to metastasize [1, 2]. Non-small cell lung cancer (NSCLC), accounting for the largest proportion (85%) of all lung cancers, displays high incidence of distant metastasis with a dismal 5-year survival rate of 5% [3–5]. Therefore, there is an unmet clinical need for

comprehensive control of metastasis, which can be achieved by the elucidation of the genetic aberrations and of the underlying signaling pathways driving NSCLC metastasis.

To identify and study novel metastasis drivers we have used both *in vitro* and *in vivo* gain-of-function and loss-of-function screens [6–10]. Using *in vitro* and *in vivo* positive selection screens, we recently identified a number of putative driver genes of lung cancer progression and metastasis, including the Mitogen Associated Protein 3 Kinase 12 Binding Inhibitory Protein (MBIP) [6, 7]. MBIP is a member of the mitogen-activated protein kinase kinase kinase (MAP3K) family [11]. MBIP contains two tandemly orientated leucine-zipper-like motifs and plays a critical role of inhibiting MAP3K12 activity to regulate JNK/SAPK signaling [12]. In addition, MBIP is part of the Ada2A Containing complex (ATAC), associated with histone modification and activation of signaling pathways [13, 14]. A recent study demonstrated that MBIP is frequently amplified in lung adenocarcinoma (LUAD) [15]. Emerging evidence indicates that MBIP expression is associated with T staging and tumor growth in patients with papillary thyroid carcinoma (PTC) [16]. Multiple studies also demonstrate MBIP interaction with other proteins, altering the expression of cancer related genes and regulating a variety of physiological processes [17, 18]. Despite its well documented role and amplification status, the mechanistic implications of MBIP in NSCLC metastasis remains elusive.

To explore the role of MBIP in metastasis, we employed a genetically-engineered $Kras^{G12D}/p53^{R172H\ G}$ murine model previously generated by our group [19]. $Kras^{G12D}$ mice develop lung adenocarcinomas that do not metastasize [20]. However, in combination with *p53* mutation, metastases are frequent at sites often observed in NSCLC [19, 21, 22]. We utilized a panel of lung adenocarcinoma cell lines derived from the $Kras^{LA1/+};p53^{R172H\ G}$ mice (KP cell line panel) [23]. These cell lines can be distinguished based on their metastatic ability, their epithelial or mesenchymal status, and their ability to undergo epithelial-to-mesenchymal transition (EMT). We have observed that the non-metastatic cells are epithelial whereas the metastatic cells have mesenchymal characteristics. (e.g., 393P is epithelial and non-metastatic, and 344SQ is highly metastatic and mesenchymal [23, 24]). We examined the expression of MBIP in publicly available databases. Moreover, we manipulated its expression in NSCLC cell lines, and found that expression of MBIP is associated with proliferation, invasion and metastasis. MBIP enhanced the migratory and invasive ability of NSCLC cells *in vitro* and metastatic capability *in vivo*. We demonstrate that MBIP exerts its metastatic effect by increasing the expression of MMPs via the activation of the JNK signaling pathway. Overall, our findings reveal a novel role for MBIP as a driver of metastasis and establish it as a potential candidate therapeutic target for metastatic NSCLC.

RESULTS

MBIP is highly amplified in Lung Adenocarcinoma and other cancers

To explore whether MBIP plays a role in NSCLC metastasis, we first examined The Cancer Genome Atlas (TCGA) database (https://www.cbioportal.org) for LUAD (provisional), to compare the ranking of genetic alterations from our previously identified driver screen [7]. We observed an overlap in genetic alterations of the top metastasis drivers with *KRAS* and

TP53. MBIP alterations occurred in 21% of cases, largely consisting of amplification, high mRNA expression and a few cases harboring missense mutations. We further analyzed its expression across cancer types in the TCGA database (Figure 1A). MBIP is amplified and displays elevated mRNA levels in lung adenocarcinomas compared with multiple cancer types, further suggesting that MBIP is essential for NSCLC (Figures 1B and Figure S1A). These results were further validated using Oncomine (Thermo Fisher Scientific) analysis which demonstrated that MBIP mRNA levels were significantly higher in LUAD compared with normal lung tissues (Figure 1C). We also assessed the expression of MBIP in the murine KP cell line panel and observed increased MBIP expression in the metastatic mesenchymal cell lines compared to the non-metastatic epithelial lines (Figure S1B). Taken together, these findings suggest that the amplification of MBIP may participate in the progression of NSCLC metastasis.

MBIP is sufficient to drive proliferation, migration and invasion of NSCLC cells *in vitro* and metastasis *in vivo*

Based on our prior screen results [6, 7] and the *in silico* findings, we hypothesized that MBIP amplification may participate in controlling cellular migration and invasion to drive metastasis. To test this hypothesis, we generated murine 393P, 344SQ, 531LN3 and human H157 lung cancer cell lines with doxycycline inducible MBIP expression. We verified the RNA and protein expression of MBIP in these cells by RT-qPCR and western blotting, respectively (Figures 2A–B and Figure S2A–B). To assess whether increased MBIP expression enhances proliferation, we performed MTT assays, which revealed an increased proliferation of MBIP overexpressing cells compared with the mCherry controls (Figure 2C). We validated these results using immunofluorescence staining for Ki67, which demonstrated robust increase in Ki67 staining in cells constitutively overexpressing MBIP (Figure S2C).

To further explore the functional role of MBIP in migration, we performed scratch-wound healing assays. Cells were incubated with 4 μM mitomycin-C, which inhibited mitosis and allowed us to distinguish migration from proliferation. We observed that overexpression of MBIP efficiently enhanced the speed of wound closure in cells with induced or constitutive MBIP overexpression, when compared with the respective control groups (Figure S2D). Consistent with these findings, Transwell chamber assays for migration and invasion revealed that elevated expression of MBIP, significantly promoted the migratory and invasive characteristics (Figure 2D and Figure S2E–F). We next examined whether MBIP affects invasion in 3D, by using a matrix comprised of Matrigel and reduced collagen, which is another determinant phenotype of metastatic cancer cell. Induction of MBIP in all the cell lines tested, showed significant increase in the number of invasive spheroid structures formed in the Matrigel/collagen matrix, suggesting that MBIP overexpression in NSCLC cells enhances invasion (Figure 2E and Figure S2G–H). EMT has been demonstrated to be a driving mechanism for migratory and invasive phenotypes in lung cancer cells. Therefore, we assessed the expression of EMT markers in mouse and human NSCLC cells upon induced expression of MBIP and observed that MBIP overexpression was able to promote EMT by upregulating Zeb1, N-Cadherin and Vimentin and downregulating E-Cadherin (Figure S2I–J).

To establish whether MBIP is sufficient to drive metastasis *in vivo,* we performed two complementary experiments. To do these, we confirmed constitutive overexpression of MBIP in the non-metastatic 393P cells by RT-qPCR and western blot analysis (Figure S2K–L). Subsequently, 1×10^6 393P cells stably overexpressing MBIP or mCherry controls were injected subcutaneously into the flanks of syngeneic WT mice and tumors measured every week, where we observed a significant increased tumor growth-rate for the MBIP overexpressing cohort (Figure 2F). Four weeks after implantation, tumors were harvested and weighed, and we observed consistent significant increase in primary tumor weights in the MBIP overexpressing tumors compared to mCherry controls (Figure 2G). To confirm that primary tumor burden was not the determinant factor, we performed a complimentary experiment where we established size-matched primary tumors in both cohorts by injecting 1×10^6 mCherry expressing control 393P cells or 5×10^5 MBIP-overexpressing 393P cells in syngeneic mice. Tumor growth-rate was monitored and observed to be indifferent between both cohorts over time and upon sacrifice (Figure S2M–N).However, mice implanted with MBIP-overexpressing cells in both the experiments, formed significantly more metastatic nodules in the lungs and visible metastatic nodules in the adrenal glands, liver, chest wall and pancreas as compared to the mice implanted with mCherry control cells, which were completely free of distant metastases (Figure 2H and Figure S2O). The metastatic propensity of MBIP-overexpressing cells was confirmed in the representative images of the gross lungs and H&E-stained cross sections (Figure 2I). RT-qPCR and western blot analyses were used to confirm the effective expression of MBIP in tumors (Figure 2J and 2K). Further, the MBIP overexpressing tumors also underwent EMT by upregulating Zeb1, N-Cadherin and Vimentin and downregulating E-Cadherin (Figure S2P). Collectively, these results suggest that MBIP is sufficient to promote proliferation, migration and invasion of NSCLC cells and induce metastasis *in vivo*.

MBIP is necessary for proliferation, migration, invasion and metastasis of NSCLC cells

To test the requirement for MBIP in lung cancer invasion and metastasis, we repressed endogenous MBIP expression in metastatic 344SQ cells using shRNAs (Figure 3A and 3B). By performing MTT assays we observed that MBIP depletion significantly decreased the proliferative capabilities of two cells lines generated using two independent shRNA constructs targeting different sequences on the MBIP mRNA, when compared with scramble controls (Figure 3C). Consistently, staining for Ki67 demonstrated a significant reduction of positively stained cells in the MBIP knockdown population, compared with the scramble control (Figure S3A). Next, we assessed the effect of MBIP knockdown on cell motility, migration, and invasion. As shown in Figure S3B, wound closure speed in 344SQ cells after prior mitomycin-C treatment, was noticeably attenuated in MBIP-depleted cells as compared with the scramble control cells. Similarly, the migratory and invasive characteristics of these cells were abrogated as elucidated by Transwell chamber assays (Figure 3D & S3C). Quantification of the number of invasive spheroids formed by shMBIP cells cultured in matrigel/collagen matrix, revealed significant reduction in these structures when compared with the scramble controls (Figure 3E & S3D). To test whether the *in vivo* metastasis was diminished by MBIP knockdown, we injected the scramble control or shMBIP cells in mice. The number of metastatic nodules was quantified after four weeks. We observed no significant changes in tumor volume and weight in mice inoculated with shMBIP cells

compared with scramble controls (Figure 3F and 3G). Quantification of the macroscopic metastases in the lungs revealed significantly fewer metastatic nodules present in lungs isolated from mice implanted with shMBIP cells compared to those from control mice injected with scramble control cells (Figure 3H). Gross lung images and H&E-staining confirmed the reduction in metastatic nodules (Figure 3I). RT-qPCR and western blotting demonstrated that MBIP knockdown levels were maintained in the tumors in comparison with their scramble controls (Figure 3J and 3K). Taken together, these results demonstrate that MBIP is necessary for cellular migration and invasion *in vitro* and for metastasis *in vivo*.

MBIP activates the JNK pathway to stimulate downstream transcription

It had been previously established that MBIP binds to and inhibits MAP3K12 activity and was shown to possibly regulate JNK signaling [12]. Therefore, to evaluate the mechanistic role of MBIP in regulation of lung cancer metastasis, we hypothesized that MBIP may activate JNK and its downstream substrates to induce metastatic events. To test this hypothesis, we performed western blot analysis, which revealed that induction of MBIP in the inducible 393P and H157 cells with doxycycline, effectively increased the phosphorylation of JNK (Figure 4A–B), without altering the total JNK levels. To determine which downstream target pathway of JNK signaling is required for the observed phenotypes in NSCLC cells, we performed western blot analysis, which showed that MBIP overexpression strongly increased the phosphorylation of c-Jun (Figure 4A–B). Conversely, depletion of MBIP in 344SQ cells impaired JNK phosphorylation, as well as the phosphorylation of c-Jun, suggesting a role for JNK activation in the causation of MBIP-mediated functional phenotypes (Figure 4C and 4F). Consistently, the transcript levels of c-Jun and its targets, Smad4, Sp1, At2 and Pax6 as determined using RT-qPCR, were significantly enriched in MBIP-overexpressing cells and repressed in MBIP-depleted cells, suggesting that MBIP may regulate downstream substrates of JNK (Figure 4D and 4E). We next tested whether JNK inhibition by a specific inhibitor, SP600125, in MBIP induced cells also affect downstream substrates and cellular phenotypes. SP600125 strongly decreased the phosphorylation of JNK and of c-Jun (Figure 4F) in the mouse 393P and human H157 cells with induced expression of MBIP. SP600125 treatment of the MBIP overexpressing cells also reverted the increased expression of c-Jun targets (Figure S4A). JNK inhibition also resulted in concomitant and significant abrogation of migration and invasion in Transwell assays (Figure 4G) and significant reduction in formation of invasive spheroids in 3D Matrigel/collagen cultures (Figure 4H). The activation of JNK by MBIP overexpression, along with decreased migration and invasion upon inhibition of JNK activity by SP600125 treatment, demonstrates the involvement of JNK signaling in MBIP–mediated migration, invasion and metastasis. Next, we specifically inhibited JNK expression in cells with induced MBIP expression using siRNAs (Figure S4B). JNK inhibition resulted in a reversal of the elevated expression of c-Jun targets and also induced partial mesenchymal-to-epithelial-transition (MET)-like molecular changes in the MBIP overexpressing cells (Figure S4C). JNK inhibition also resulted in a significant decrease in the migratory and invasive capabilities of the MBIP expressing cells however, there was no change in cell proliferation (Figure S4D–E).

MBIP induces cellular invasion by upregulating matrix metalloproteinases upon activation of JNK signaling

JNK activates the AP-1 transcription factor family [25], which regulates expression of genes involved in cancer progression, including matrix metalloproteinases (MMPs). MMPs are a family of proteins that degrade extracellular matrix (ECM) to promote tumor cell migration, invasion, metastasis, apoptosis and carcinogenesis [26, 27]. Since MBIP overexpression activated JNK signaling and also induced cellular migration and invasion in 2D and also formation of invasive spheroids in 3D matrices, we hypothesized that MBIP may control the expression of MMPs. The mRNA levels of MMPs (MMP1, MMP2, MMP3, MMP7, MMP9 and MMP13) were evaluated by RT–qPCR analysis. Overexpression of MBIP in 393P and H157 cells significantly increased the mRNA expression of MMP7, with several other MMPs also showing robust increases such as MMP1, MMP9 and MMP13 (Figure 5A & S5A). Conversely, when MBIP was repressed in the metastatic 344SQ cells, multiple MMP mRNA levels were decreased, including MMP7 (Figure 5B & S5A). These results suggested that MMPs may play a prominent role as a downstream effector of the MBIP/JNK axis. Consistent with the hypothesis, mRNA expression of MMPs was significantly abrogated following SP600125 treatment in both murine and human MBIP overexpressing cells (Figure 5C). Collectively, these results suggest that MBIP promotes the expression of multiple MMPs by activating JNK phosphorylation, leading to an increased migration and invasion capacity of NSCLC cells.

Pharmacological inhibition of MMP impairs NSCLC cells migration and invasion *in vitro*

To further explore how MMPs modulate the phenotypes associated with the MBIP/JNK axis, we used GM6001, a broad-spectrum MMP inhibitor, to pharmacologically inhibit MMP activity in 393P and H157 models and evaluated the effects on cellular migration and invasion. Transwell chamber migration assays using MBIP-overexpressing cells showed that GM6001 treatment significantly suppressed cell migration and invasion compared to DMSO treated cells (Figure. 5D). Consistently, GM6001 treatment decreased formation of invasive structures in Matrigel/collagen matrix compared to DMSO-treated cells (Figure 5E). To further confirm the functional effect of MMPs downstream of MBIP overexpression, we independently inhibited the expression of MMP1a, MMP2, or MMP7 in MBIP overexpressing cells or vector controls, using targeted siRNA pools (Figure S5B). Knockdown of each MMP in the MBIP overexpressing cells resulted in significant reduction of migratory and invasive properties of these cells in 2D (Figure S5C) and also a significant reduction in invasive structures formed in 3D matrix (Figure S5D). However, there was no observable change in cellular proliferation (Figure S5E). These results strongly suggested that MMP activity is responsible for MBIP-mediated cellular migration and invasion.

Next, we used immunohistochemistry analysis to examine the activity of the MBIP/JNK/MMP axis *in vivo.* IHC revealed a positive correlation of MBIP with an increase in phosphorylated JNK, phosphorylated–c-Jun and MMP7 levels in MBIP-overexpressing tumors and scramble control tumors (Figure 6A–B and Figure S6A–B), but not in the MBIP depleted or mCherry control tumors. Since we had observed that MBIP expression could significantly alter MMP transcriptional levels (Figure 5A–C), we therefore analyzed MMP

expression in the tumors generated from MBIP overexpressing or MBIP depleted cells and their respective control cohorts. MBIP overexpression resulted in significant upregulation of MMP1a, MMP2, MMP7 and MMP9 when compared to mCherry expressing control tumors *in vivo*. Conversely, these MMPs were significantly downregulated in the MBIP depleted tumors when compared to the scramble control tumors (Figure S6C). Further, in the lung tissues with high incidence of metastatic lesions in the MBIP overexpressing and the scramble control cohorts, elevated expression of p-JNK, p-c-Jun and MMP7 immuno-positive cells were detected compared to the lung tissue without metastasis from the mCherry control and MBIP depleted cohorts. To confirm these results, we performed a western blot analysis on protein from tumors from the different cohorts. We observed (Figure 6C) a similar activation of JNK and c-Jun as demonstrated by their phosphorylation levels, in the 393P-MBIP-overexpressing tumors and the 344SQ-scramble control tumors. Furthermore, the protein expression of MMP7 was also significantly elevated in these tumor lysates. Tumor lysates from MBIP depleted tumors (344SQ-shMBIP#5) as well as the mCherry control tumors, demonstrated reduced phosphorylation levels of JNK, c-Jun and reduced expression of MMP7. Taken together, these results suggest that MBIP could activate JNK signaling *in vivo,* that induces phosphorylation of JNK and activation of MMPs, which plays an important role in MBIP mediated tumor growth, invasion and metastasis in NSCLC.

Discussion

There is an urgent unfulfilled need to find novel therapeutically targetable drivers for lung cancer metastasis since the clinical options for treatment of metastatic NSCLC are still largely limited. As a follow-up study to our recent *in vitro* and *in vivo* gain-of-function screens that identified potential genes promoting invasion and metastasis, here we investigated the mechanistic and clinical relevance of MBIP in the context of NSCLC metastasis [6, 7]. MBIP has been reported to be clinically associated with papillary thyroid cancer T staging and its genomic amplification has been found in significant proportions of lung adenocarcinomas in combination with other drivers like NKX2–1 [15, 16, 28]. In concurrence with this, here we examined the TCGA database and confirmed that MBIP is highly amplified in lung adenocarcinomas as well as in various other cancer types when compared to normal tissues. This is also the first report whereby using multiple complementary approaches we have elucidated a comprehensive mechanistic role of MBIP as a driver of cellular proliferation, migration, invasion and metastasis in NSCLC.

MBIP has been demonstrated as an upstream inhibitor of MAP3K12 activity and has been shown to modestly inhibit JNK signaling in non-cancerous cells [12, 29], though functional consequences of MBIP-mediated regulation of the JNK/SAPK pathways in a cancer context has been understudied. Here, we convincingly demonstrate that in Kras/p53 mutated lung cancer models, MBIP could strongly induce the activation of JNK/SAPK pathway. The oncogenic role of JNK is dependent on its ability to phosphorylate c-Jun and to activate AP-1 in response to an extracellular stimulus [32, 33]. In this study, we provide evidence that MBIP overexpression leads to increased phosphorylation of JNK in NSCLC cells which in turn results in functional activation of c-JUN and also induces EMT-like molecular changes. In addition, MBIP-induced migration, invasion and c-JUN activity was

significantly reduced upon JNK inhibition by using SP600125. This observation suggests that JNK activation is crucial in MBIP-mediated NSCLC cell invasion and metastasis. We also confirmed these finding by elucidating that in MBIP depleted cells JNK/c-JUN activity was severely compromised with decreased invasion and metastatic progression *in vivo*.

Our data demonstrating reduced number of lung metastatic nodules from MBIP deficient cells suggest that MBIP promotes metastatic process and its amplification could be an important cause of NSCLC spread. We also indicated that phosphorylation of JNK was a significant step in metastatic progression. Knockdown of MBIP resulted in an inactive JNK signaling *in vitro* and *in vivo*, suggesting that activation of JNK signaling is essential for the disseminated tumor cells to establish metastases to distant organs. This notion is consistent with the findings of a previous study which showed that JNK activation can induce proliferation and tumorigenesis of cancer cells [30]. Another study also showed using gastric cancer mouse model, that metastasis can be mediated by JNK signaling pathway [31]. Therefore, it is possible that MBIP expression in primary tumors activates the JNK signaling machinery, which induces migration and drives invasion to allow metastatic colonization. However, future efforts are warranted to decipher how the ATAC complex may regulate or influence MBIP induced processes, which may deepen our understanding of this gene function in NSCLC progression and metastasis and may result in developing it as target for personalized treatment of NSCLC.

We reconciled our mechanistic studies by investigating the downstream targets of JNK-dependent transcription factors in different scenarios. It has been established that JNK signaling regulate MMPs [32, 33]. In our present study, we revealed that MBIP participates in activation of matrix metalloproteinase (MMPs) in NSCLC cells. MMPs are a family of zinc-dependent endopeptidases involved in degrading ECM to facilitate tumorigenesis and metastasis [34–39]. MMPs are secreted by epithelial cells and has been shown to promote cellular invasion [40, 41]. Additionally, recent studies have shown that expression of MMPs contributes to tumor proliferation, invasion, and poor prognosis in NSCLC patients [42, 43]. Here we provided evidence that mRNA expression of MMP1a, MMP2, MMP7 and MMP9 is significantly induced by MBIP overexpression in cells. Since MMP regulation occurs primarily at the transcription level [44, 45], our data suggest that MBIP could affect transcriptional or post-transcriptional mechanisms to modify MMP expression. The increase in MMP levels is required for cell migration and invasion *in vitro* as inhibition of MMPs using the broad spectrum MMP inhibitor (GM6001) in the MBIP-overexpressing cells results in a reversal of these phenotypes. This suggests that the increased robust metastatic phenotype, observed upon MBIP expression, requires the expression of MMPs, which is consistent with previous findings on the role of MMPs in metastatic spread [46]. In this study we show for the first time that MBIP could function as an upstream regulator of MMP activity and secretion, by which it could induce increased cellular migration, invasion and metastasis in NSCLC.

In conclusion, this study is the first to report that the MBIP promotes NSCLC invasion and metastasis. We highlighted a novel role for MBIP as a driver gene activating MMP expression by elucidating a mechanistic insight of MBIP-mediated regulation of JNK/c-JUN axis to promote invasion and metastasis of NSCLC cells (Figure 6D). We propose that MBIP

may serve as potential prognostic indicator in NSCLC metastasis, and as a therapeutic target for treatment of metastatic disease.

Materials and Methods

Additional experimental details in supplemental methods. N=3 unless specified as it is the minimum requirement for performing a Student's T-test. Data are represented as mean ± SEM. Significance by Student's T-test. Variance is not equal, so we use parametric t-test. P-value<0.05 - *; <0.002 - **

Cell culture—All cell lines were maintained in RPMI-1640 supplemented with 10% fetal bovine serum and propagated at 37 °C and 5% CO_2 in humidified atmosphere. Murine cell lines were generated and characterized in our lab and tested mycoplasma negative [23]. H157 cells were procured from ATCC.

Constructs and reagents—MBIP knockdown and overexpressing cells were generated by Lentiviral transduction of parental cell lines followed by Puromycin selection. For shRNA knockdowns, constructs were purchased from Horizon, USA. For generating inducible MBIP construct, mouse MBIP cDNA was cloned (EcoRI and XhoI) in a doxycycline inducible lentiviral construct as described before [9]. The constitutively over-expressing MBIP construct and the mCherry control construct was generated as described before [7]. shRNA and siRNA details in supplemental methods.

Wound healing assay—Cells were seeded into a 6-well plate and cultured to confluency with complete medium. A 200μl tip (1 mm) was used to make a scratch on the cell monolayer as previously described [47]. Then the cells were washed with PBS and incubated with 4μM mitomycin C for 24 h. Percentage wound healing was calculated by comparing area migrated between 0 and 24 hours by experimental cells compared to control. N=3 images/well and 2 wells/sample. All data were analyzed from three independent experiments performed in triplicate and the results are expressed as the mean ± SD.

Migration and invasion assay—Migration and invasion assays were performed as described previously [9]. Briefly, Transwell chamber (8 μm pore polycarbonate, Corning Costar, USA) coated with the diluted BD Matrigel™ basement membrane matrix (BD Biosciences, Bedford, MA, USA) were used. Cells treated with doxycycline (0–5μM) for 24h were plated at 5×10^4 cells/chamber in serum-free RPMI medium for 16 hours. Migrated/invaded cells were stained and quantified. Details included in supplementary methods.

Animal studies—All animal experiments were in accordance with the Institutional Animal Care and Use Committee (IACUC) at The University of Texas M.D. Anderson Cancer Center. Cells were subcutaneously implanted in the flanks of syngeneic 129/sv male and female mice. Tumor volume was monitored twice a week for tumor growth for a period of four weeks. Tumors were measured and calculated by length × width^2/2. Upon euthanasia by using CO_2, lung macro-metastatic nodules were counted. Lung tissue was fixed in 10% formalin and processed for sectioning followed by H&E staining. Power analysis for sample size determination using 80% power and 5% two-sided type 1 error.

RT–qPCR and western blot—mRNA levels were determined by RT-qPCR, as previously described [9]. RNA from the cells transfected with each construct or tissue samples from tumors was isolated using TRIzol® (Invitrogen, USA). To obtain cDNA, the isolated RNA (2 ng/μl) was reverse transcribed using qScript™ (030497, Quanta Bio, USA) as previously described [7, 9]. Primer details in supplemental methods. Western blot was performed with antibodies mentioned in supplemental methods.

Immunohistochemistry—Formalin-fixed, paraffin-embedded specimens were cut into 4μm-thick sections. The sections were dewaxed in xylene and rehydrated stepwise in descending ethanol series. Antigen retrieval was performed using citric acid (s1399, Dako, USA). Endogenous peroxidase activity and non-specific binding were blocked with 3% H_2O_2. The sections were then incubated with primary overnight at 4°C and then incubated with secondary antibody for 1 hour at RT. Immunohistochemistry was carried out using the Envision+ System (DAKO), Streptavidin (DAKO) and HRP-DAB colorimetric detection. Secondary antibodies against the correct IgG species were conjugated with peroxidase (Dako). Antibody details in supplemental methods.

Immunofluorescence (IF) staining for EMT markers—For IF staining studies, cells were fixed with 4% paraformaldehyde for 20 min, permeabilized in 0.5% Triton X-100 for 10 min, washed three times with PBS, and blocked in IF buffer (PBS, 0.1 % BSA, 0.2 % Triton X-100, and 0.05 % Tween-20) containing 10 % FBS at 37°C for 30 min. Cells were stained with primary antibody against MBIP, Ki67 overnight at 4°C, and washed three times with TBST. After being incubated with Alexa 488-conjugated secondary antibodies (Invitrogen) and counterstaining with 4′,6-diamidino-2-phenylindole (DAPI), slides were mounted with VECTASHIELD Hard-Set Mounting Medium (Vector Laboratories, Burlingame, CA). Fluorescent images were visualized using an Olympus IX71 fluorescence microscope (Olympus, Japan). Antibody details in supplemental methods.

Cell assay (3D culture)—Three-dimensional (3D) cultures were conducted, as previously described [23]. Mixture of Matrigel (BD Biosciences) and Collagen (Corning) plated in eight-well chambered glass slides (Nunc, Naperville, IL) were used to grow cells in complete media with 2% Matrigel, which was changed every 2–3 d. Details included in supplementary methods.

Supplementary Material

Refer to Web version on PubMed Central for supplementary material.

Acknowledgements

Reference

1. Siegel RL, Miller KD, Jemal A. Cancer statistics, 2019. CA Cancer J Clin 2019; 69: 7–34. [PubMed: 30620402]

2. Sporn MB. The war on cancer. Lancet 1996; 347: 1377–1381. [PubMed: 8637346]

3. Zappa C, Mousa SA. Non-small cell lung cancer: current treatment and future advances. Transl Lung Cancer Res 2016; 5: 288–300. [PubMed: 27413711]

4. Olaussen KA, Dunant A, Fouret P, Brambilla E, Andre F, Haddad V et al. DNA repair by ERCC1 in non-small-cell lung cancer and cisplatin-based adjuvant chemotherapy. N Engl J Med 2006; 355: 983–991. [PubMed: 16957145]

5. Jamal-Hanjani M, Wilson GA, McGranahan N, Birkbak NJ, Watkins TBK, Veeriah S et al. Tracking the Evolution of Non-Small-Cell Lung Cancer. N Engl J Med 2017; 376: 2109–2121. [PubMed: 28445112]

6. Bajaj R, Kundu ST, Grzeskowiak CL, Fradette JJ, Scott KL, Creighton CJ et al. IMPAD1 and KDELR2 drive invasion and metastasis by enhancing Golgi-mediated secretion. Oncogene 2020 (In Press).

7. Grzeskowiak CL, Kundu ST, Mo X, Ivanov AA, Zagorodna O, Lu H et al. In vivo screening identifies GATAD2B as a metastasis driver in KRAS-driven lung cancer. Nat Commun 2018; 9: 2732. [PubMed: 30013058]

8. Konen JM, Rodriguez BL, Fradette JJ, Gibson L, Davis D, Minelli R et al. Ntrk1 Promotes Resistance to PD-1 Checkpoint Blockade in Mesenchymal Kras/p53 Mutant Lung Cancer. Cancers (Basel) 2019; 11.

9. Kundu ST, Grzeskowiak CL, Fradette JJ, Gibson LA, Rodriguez LB, Creighton CJ et al. TMEM106B drives lung cancer metastasis by inducing TFEB-dependent lysosome synthesis and secretion of cathepsins. Nat Commun 2018; 9: 2731. [PubMed: 30013069]

10. Peng DH, Kundu ST, Fradette JJ, Diao L, Tong P, Byers LA et al. ZEB1 suppression sensitizes KRAS mutant cancers to MEK inhibition by an IL17RD-dependent mechanism. Sci Transl Med 2019; 11.

11. Inoue H, Tateno M, Fujimura-Kamada K, Takaesu G, Adachi-Yamada T, Ninomiya-Tsuji J et al. A Drosophila MAPKKK, D-MEKK1, mediates stress responses through activation of p38 MAPK. EMBO J 2001; 20: 5421–5430. [PubMed: 11574474]

12. Fukuyama K, Yoshida M, Yamashita A, Deyama T, Baba M, Suzuki A et al. MAPK upstream kinase (MUK)-binding inhibitory protein, a negative regulator of MUK/dual leucine zipper-bearing kinase/leucine zipper protein kinase. J Biol Chem 2000; 275: 21247–21254. [PubMed: 10801814]

13. Suganuma T, Gutierrez JL, Li B, Florens L, Swanson SK, Washburn MP et al. ATAC is a double histone acetyltransferase complex that stimulates nucleosome sliding. Nat Struct Mol Biol 2008; 15: 364–372. [PubMed: 18327268]

14. Guelman S, Kozuka K, Mao Y, Pham V, Solloway MJ, Wang J et al. The double-histone-acetyltransferase complex ATAC is essential for mammalian development. Mol Cell Biol 2009; 29: 1176–1188. [PubMed: 19103755]

15. Weir BA, Woo MS, Getz G, Perner S, Ding L, Beroukhim R et al. Characterizing the cancer genome in lung adenocarcinoma. Nature 2007; 450: 893–898. [PubMed: 17982442]

16. Jendrzejewski J, Liyanarachchi S, Nagy R, Senter L, Wakely PE, Thomas A et al. Papillary Thyroid Carcinoma: Association Between Germline DNA Variant Markers and Clinical Parameters. Thyroid 2016; 26: 1276–1284. [PubMed: 27342578]

17. Levin PA, Brekken RA, Byers LA, Heymach JV, Gerber DE. Axl Receptor Axis: A New Therapeutic Target in Lung Cancer. J Thorac Oncol 2016; 11: 1357–1362. [PubMed: 27130831]

18. Lee YH, Kim JH, Song GG. Genome-wide pathway analysis of breast cancer. Tumour Biol 2014; 35: 7699–7705. [PubMed: 24805830]

19. Gibbons DL, Lin W, Creighton CJ, Zheng S, Berel D, Yang Y et al. Expression signatures of metastatic capacity in a genetic mouse model of lung adenocarcinoma. PLoS One 2009; 4: e5401. [PubMed: 19404390]

20. Johnson L, Mercer K, Greenbaum D, Bronson RT, Crowley D, Tuveson DA et al. Somatic activation of the K-ras oncogene causes early onset lung cancer in mice. Nature 2001; 410: 1111–1116. [PubMed: 11323676]

21. Zhu J, Zheng Y, Zhang H, Liu Y, Sun H, Zhang P. Galectin-1 induces metastasis and epithelial-mesenchymal transition (EMT) in human ovarian cancer cells via activation of the MAPK JNK/p38 signalling pathway. Am J Transl Res 2019; 11: 3862–3878. [PubMed: 31312395]

22. Zheng S, El-Naggar AK, Kim ES, Kurie JM, Lozano G. A genetic mouse model for metastatic lung cancer with gender differences in survival. Oncogene 2007; 26: 6896–6904. [PubMed: 17486075]

23. Gibbons DL, Lin W, Creighton CJ, Rizvi ZH, Gregory PA, Goodall GJ et al. Contextual extracellular cues promote tumor cell EMT and metastasis by regulating miR-200 family expression. Genes & development 2009; 23: 2140–2151. [PubMed: 19759262]

24. Ahn YH, Gibbons DL, Chakravarti D, Creighton CJ, Rizvi ZH, Adams HP et al. ZEB1 drives prometastatic actin cytoskeletal remodeling by downregulating miR-34a expression. The Journal of clinical investigation 2012; 122: 3170–3183. [PubMed: 22850877]

25. Gazon H, Barbeau B, Mesnard JM, Peloponese JM Jr. Hijacking of the AP-1 Signaling Pathway during Development of ATL. Front Microbiol 2017; 8: 2686. [PubMed: 29379481]

26. McCawley LJ, Matrisian LM. Matrix metalloproteinases: multifunctional contributors to tumor progression. Mol Med Today 2000; 6: 149–156. [PubMed: 10740253]

27. Basu S, Thorat R, Dalal SN. MMP7 is required to mediate cell invasion and tumor formation upon Plakophilin3 loss. PLoS One 2015; 10: e0123979. [PubMed: 25875355]

28. Harris T, Pan Q, Sironi J, Lutz D, Tian J, Sapkar J et al. Both gene amplification and allelic loss occur at 14q13.3 in lung cancer. Clin Cancer Res 2011; 17: 690–699. [PubMed: 21148747]

29. Suganuma T, Mushegian A, Swanson SK, Abmayr SM, Florens L, Washburn MP et al. The ATAC acetyltransferase complex coordinates MAP kinases to regulate JNK target genes. Cell 2010; 142: 726–736. [PubMed: 20813260]

30. Sui X, Kong N, Ye L, Han W, Zhou J, Zhang Q et al. p38 and JNK MAPK pathways control the balance of apoptosis and autophagy in response to chemotherapeutic agents. Cancer Lett 2014; 344: 174–179. [PubMed: 24333738]

31. Choi Y, Ko YS, Park J, Choi Y, Kim Y, Pyo JS et al. HER2-induced metastasis is mediated by AKT/JNK/EMT signaling pathway in gastric cancer. World J Gastroenterol 2016; 22: 9141–9153. [PubMed: 27895401]

32. Ispanovic E, Haas TL. JNK and PI3K differentially regulate MMP-2 and MT1-MMP mRNA and protein in response to actin cytoskeleton reorganization in endothelial cells. Am J Physiol Cell Physiol 2006; 291: C579–588. [PubMed: 16672691]

33. Cheng CY, Hsieh HL, Hsiao LD, Yang CM. PI3-K/Akt/JNK/NF-kappaB is essential for MMP-9 expression and outgrowth in human limbal epithelial cells on intact amniotic membrane. Stem Cell Res 2012; 9: 9–23. [PubMed: 22459175]

34. Liotta LA, Stetler-Stevenson WG. Metalloproteinases and cancer invasion. Semin Cancer Biol 1990; 1: 99–106. [PubMed: 2103492]

35. Stamenkovic I Matrix metalloproteinases in tumor invasion and metastasis. Semin Cancer Biol 2000; 10: 415–433. [PubMed: 11170864]

36. Kenny HA, Kaur S, Coussens LM, Lengyel E. The initial steps of ovarian cancer cell metastasis are mediated by MMP-2 cleavage of vitronectin and fibronectin. J Clin Invest 2008; 118: 1367–1379. [PubMed: 18340378]

37. Li M, Li P, Zhang M, Ma F. Brucine suppresses breast cancer metastasis via inhibiting epithelial mesenchymal transition and matrix metalloproteinases expressions. Chin J Integr Med 2018; 24: 40–46. [PubMed: 28795388]

38. Stanciu AE, Zamfir-Chiru-Anton A, Stanciu MM, Popescu CR, Gheorghe DC. Imbalance between Matrix Metalloproteinases and Tissue Inhibitors of Metalloproteinases Promotes Invasion and Metastasis of Head and Neck Squamous Cell Carcinoma. Clin Lab 2017; 63: 1613–1620. [PubMed: 29035450]

39. Conlon GA, Murray GI. Recent advances in understanding the roles of matrix metalloproteinases in tumour invasion and metastasis. J Pathol 2019; 247: 629–640. [PubMed: 30582157]

Author Manuscript

40. McDonnell S, Navre M, Coffey RJ Jr., Matrisian LM. Expression and localization of the matrix metalloproteinase pump-1 (MMP-7) in human gastric and colon carcinomas. Mol Carcinog 1991; 4: 527–533. [PubMed: 1793490]

41. Wang FQ, So J, Reierstad S, Fishman DA. Matrilysin (MMP-7) promotes invasion of ovarian cancer cells by activation of progelatinase. Int J Cancer 2005; 114: 19–31. [PubMed: 15523695]

42. He W, Zhang H, Wang Y, Zhou Y, Luo Y, Cui Y et al. CTHRC1 induces non-small cell lung cancer (NSCLC) invasion through upregulating MMP-7/MMP-9. BMC Cancer 2018; 18: 400. [PubMed: 29631554]

43. Liu D, Nakano J, Ishikawa S, Yokomise H, Ueno M, Kadota K et al. Overexpression of matrix metalloproteinase-7 (MMP-7) correlates with tumor proliferation, and a poor prognosis in non-small cell lung cancer. Lung Cancer 2007; 58: 384–391. [PubMed: 17728005]

44. Suminoe A, Matsuzaki A, Hattori H, Koga Y, Ishii E, Hara T. Expression of matrix metalloproteinase (MMP) and tissue inhibitor of MMP (TIMP) genes in blasts of infant acute lymphoblastic leukemia with organ involvement. Leuk Res 2007; 31: 1437–1440. [PubMed: 17350093]

45. Vincenti MP. The matrix metalloproteinase (MMP) and tissue inhibitor of metalloproteinase (TIMP) genes. Transcriptional and posttranscriptional regulation, signal transduction and cell-type-specific expression. Methods Mol Biol 2001; 151: 121–148. [PubMed: 11217296]

46. Naglich JG, Jure-Kunkel M, Gupta E, Fargnoli J, Henderson AJ, Lewin AC et al. Inhibition of angiogenesis and metastasis in two murine models by the matrix metalloproteinase inhibitor, BMS-275291. Cancer Res 2001; 61: 8480–8485. [PubMed: 11731431]

47. Martinotti S, Ranzato E. Scratch Wound Healing Assay. Methods Mol Biol 2019.

A

B

C

Fold change=2.600, p=1.37E-5, t-Test=5.664
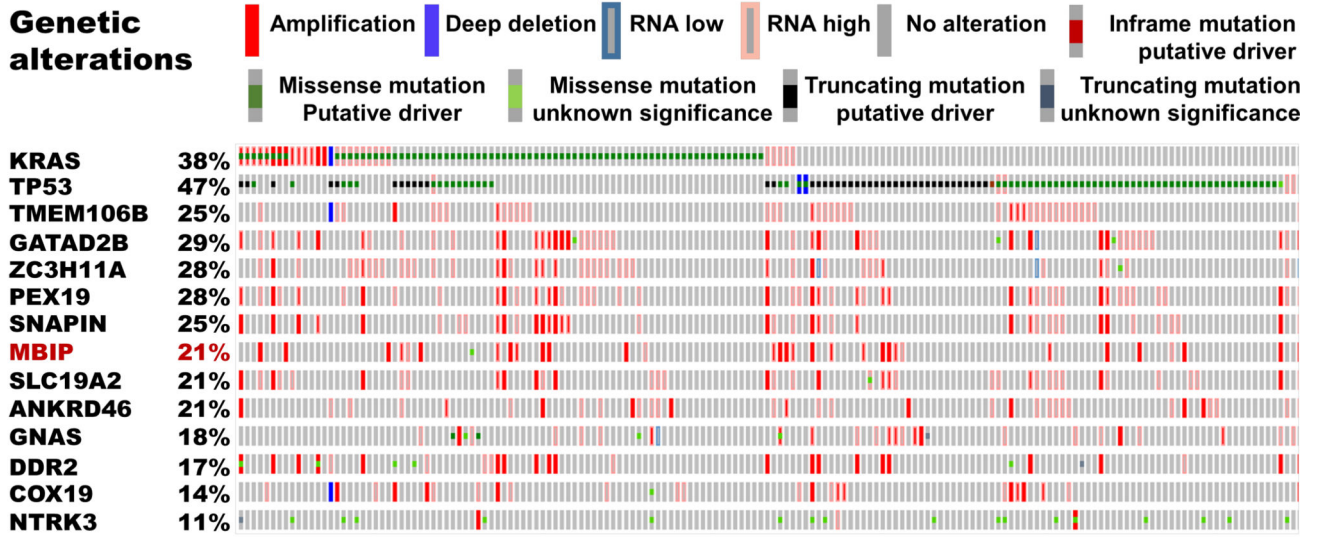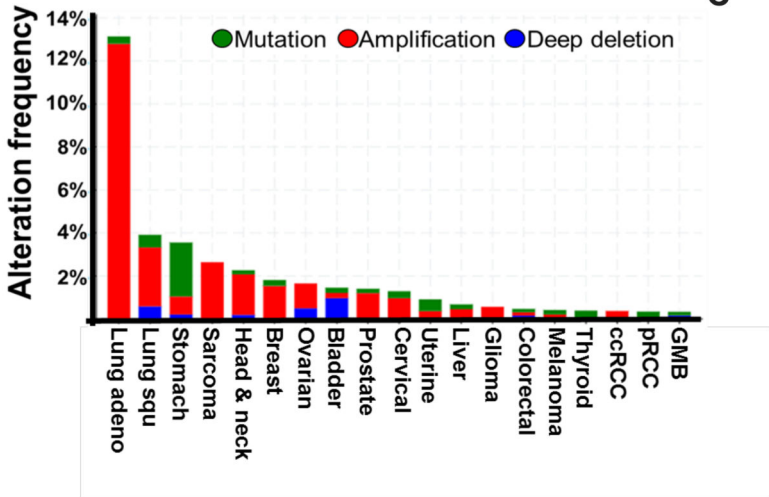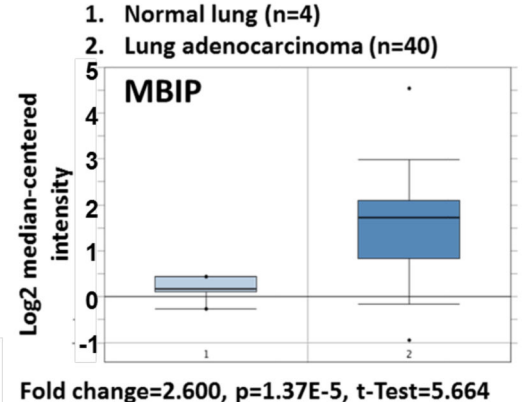
Figure 1. MBIP is highly amplified in Lung Adenocarcinoma.
(A) Oncoprint analysis in TCGA provisional LUAD dataset, showing genetic alterations in KRAS, TP53, MBIP and other metastatic drivers as identified in our previously reported *in vivo* gain of function screen [7, 9]. Amplifications (red), deletions (blue), mutations (green). **(B)** MBIP alteration frequency across cancer types in TGGA datasets. **(C)** Oncomine analysis of MBIP mRNA expression profile in lung adenocarcinoma data sets.
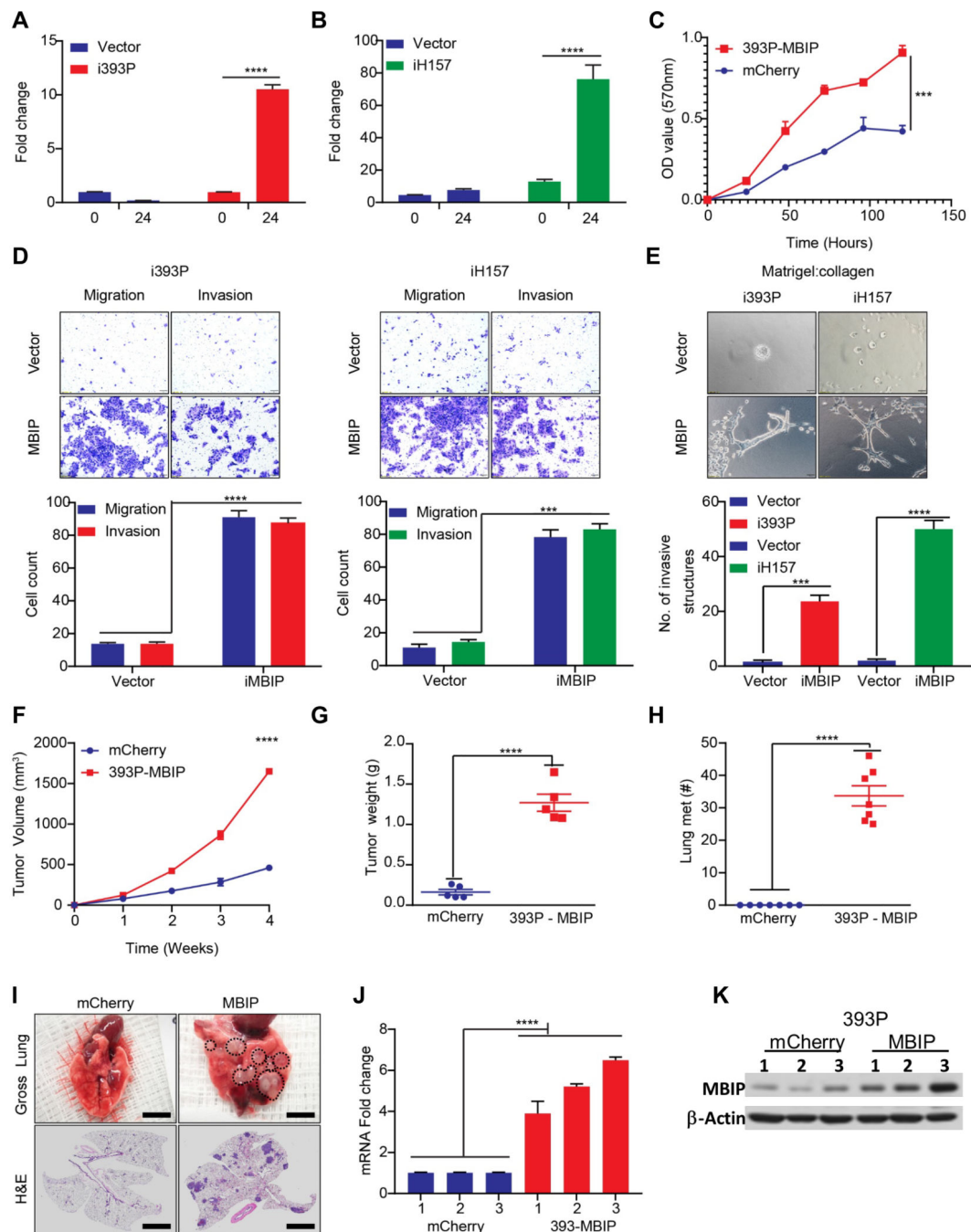
Figure 2. MBIP is sufficient to drive proliferation, migration and invasion of NSCLC cells *in vitro* and metastasis *in vivo*.
(A- B) qRT-PCR analysis to determine expression of MBIP, after 24 hours of doxycycline induction in i393P and iH157 cells with inducible expression of MBIP or GFP (vector) as controls. **(C)** Proliferation over a period of 0 – 120 hours, as determined by MTT assay using 393P cells with constitutive overexpression of MBIP or mCherry as control. Representative images of **(D)** Transwell chamber assays performed for migration and invasion or **(E)** 3D matrix (Matrigel+collagen) with invasive spheroids, formed by i393P and

iH157 cells with inducible expression of MBIP or GFP (vector) as controls. The number of cells migrated/invaded through the membrane/matrix were quantified as described in Materials and Methods. 3D matrix was comprised of Matrigel containing 1.5 mg/ml reduced collagen and imaging was performed after 120h of seeding. **(F)** Flanks of syngeneic WT mice were Implanted using 393P cells with constitutive over expression of MBIP or mCherry as controls. Tumor volumes were measured every week in the implanted mice for 4 weeks. N = 7 **(G)** Tumor weights and **(H)** counts of gross lung metastatic lesions were recorded upon sacrifice of animals at the experimental endpoint. **(I)** Representative images were taken of lungs with macroscopic metastatic lesion (upper panel) and HE stained slides (lower panel) of the lung sections. **(J)** RT-qPCR and **(K)** Western blot analysis to determine MBIP expression levels in representative primary tumors from mice as described in (F-G). Three samples were included for each group, and one representative experiment out of three is shown. ****$P < 0.0001$ is based on the Student t test. All results are from three independent experiments. Error bars represent SD.
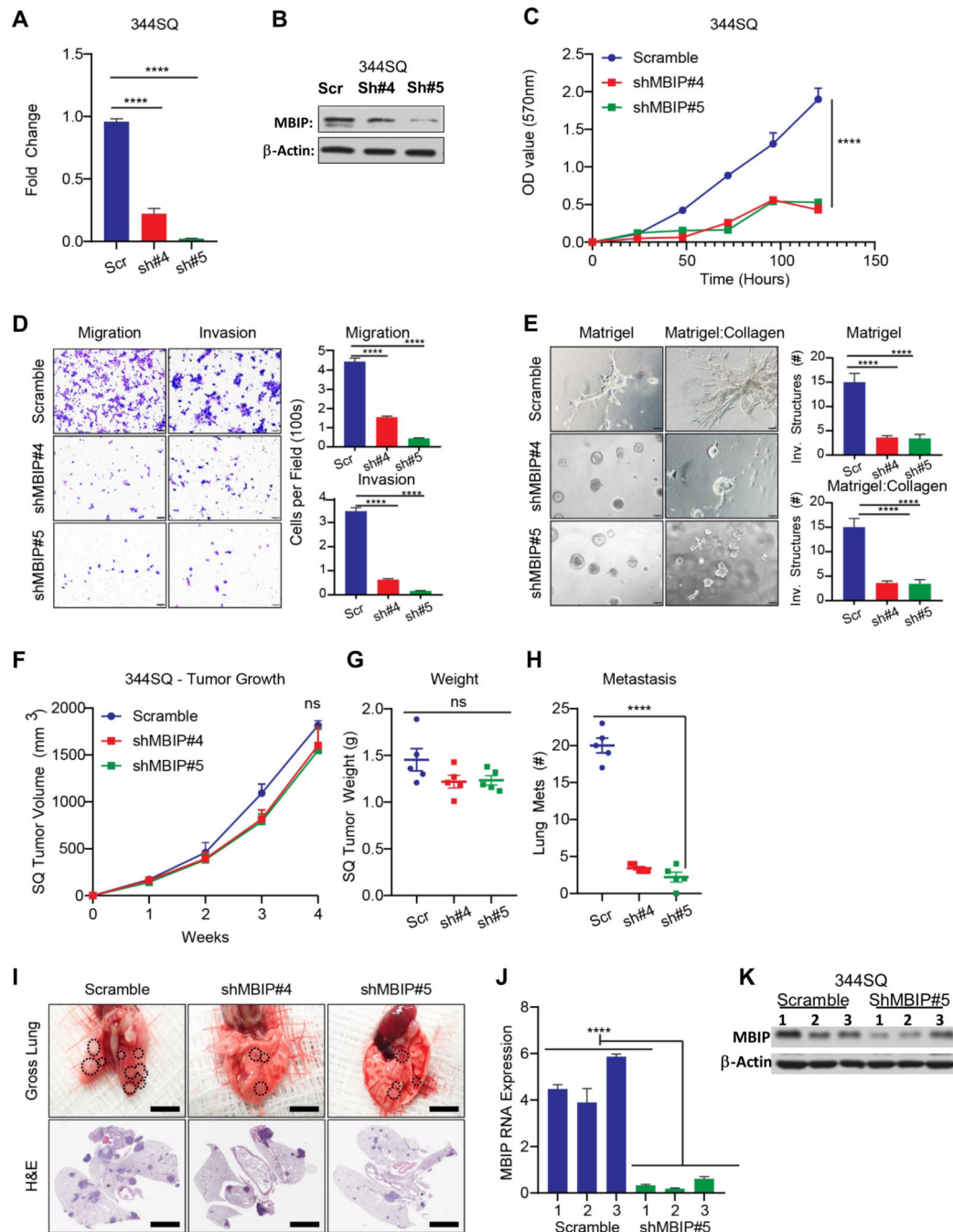
Figure 3. MBIP is necessary for proliferation, migration, invasion and metastasis of NSCLC cells.

(**A**) qRT-PCR and (**B**) Western blot analysis of 344SQ cells with stable knockdown of MBIP (344SQ-Scramble control and 344SQ-ShMBIP#4,#5) (**C**) MTT assays indicating significantly decreased proliferation in 344SQ cells with stable knockdown of MBIP. Representative images of (**D**) Transwell chamber assays performed for migration and invasion or (**E**) 3D matrix (Matrigel+collagen) with invasive spheroids, formed by 344SQ cells with stable knockdown of MBIP. (**F**) Tumor volumes were measured every week in

mice Implanted with 344SQ cells with stable knockdown of MBIP or scramble control (344SQ-Scramble control and 344SQ-shMBIP#4, #5). N = 5 **(G)** Tumor weights and **(H)** counts of gross lung metastatic lesions were recorded upon sacrifice of animals at the experimental endpoint. **(I)** Representative images were taken of lungs with macroscopic metastatic lesion (upper panel) and HE stained slides (lower panel) of the lung sections. **(J)** qRT-PCR and **(K)** Western blot analysis to determine MBIP expression levels in representative primary tumors from mice as described in (F-G). Three samples were included for each group, and one representative experiment out of three is shown. ****$P < 0.0001$ is based on the Student t test. All results are from three independent experiments. Error bars represent SD.
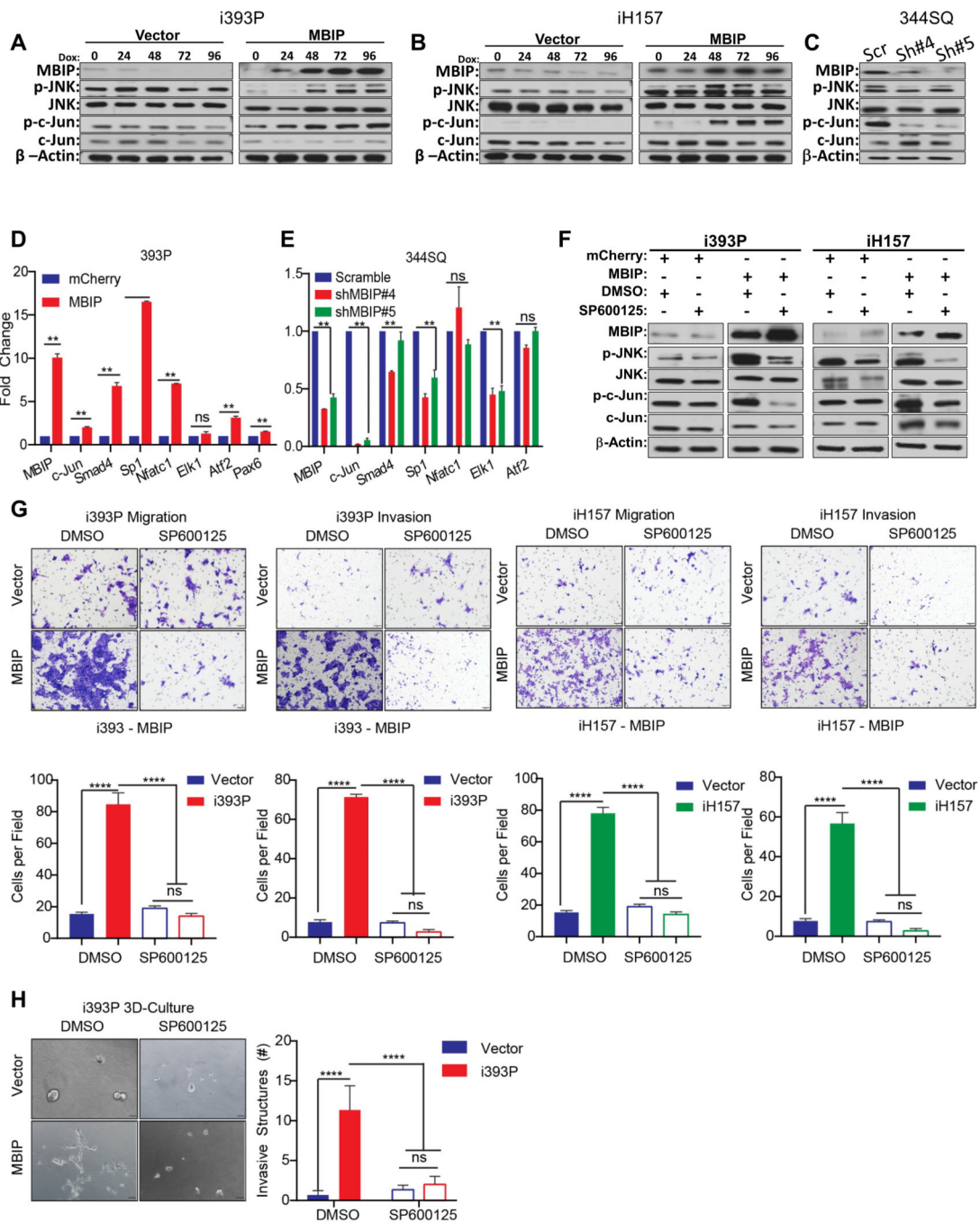
Figure 4. MBIP activates JNK pathway and regulates direct downstream targets.
30μg of a whole cell extract from (**A**) i393P and (**B**) iH157 cells with induced expression of MBIP or GFP(Vector) as control, or (**C**) MBIP knockdown (344SQ-Scramble control and 344SQ-shMBIP#4,#5) cells were resolved on 10% SDS PAGE gels followed by Western blotting with specific antibodies as indicated. Note that p-JNK and p-c-JUN levels are substantially higher in MBIP overexpressing cells and conversely lower in the MBIP knockdown cells when compared to the respective control cells. Western blots for β actin served as a loading control (lower panels). qRT-PCR analysis performed for the indicated

JNK downstream target genes, using mRNA from **(D)** 393P cells with constitutive expression of MBIP (393P-MBIP or 393P-mCherry control), or **(E)** MBIP knockdown (344SQ-Scramble control and 344SQ-ShMBIP#4, #5) cells. **(F)** Western blot analysis for indicated proteins performed on whole cell extracts from i393P and iH157 cells with induced expression of MBIP or GFP (Vector) as control, which were treated with a specific JNK inhibitor (SP600125) or DMSO as control. **(G)** Representative images of Transwell chamber assays performed for migration and invasion of i393P or iH157 cells with induced expression of MBIP or GFP (Vector) as controls, which were treated with a specific JNK inhibitor (SP600125) or DMSO as control. The number of cells migrated/invaded through the membrane/matrix were quantified as described in Materials and Methods. **(H)** Representative images of 3D matrix (Matrigel+collagen) with invasive spheroids, formed by doxycycline-inducible MBIP-overexpressing i393P cells, which were treated with a specific JNK inhibitor (SP600125) or DMSO as control. **P < 0.01, ****P < 0.0001 is based on the Student t test. All results are from three independent experiments. Error bars represent SD.
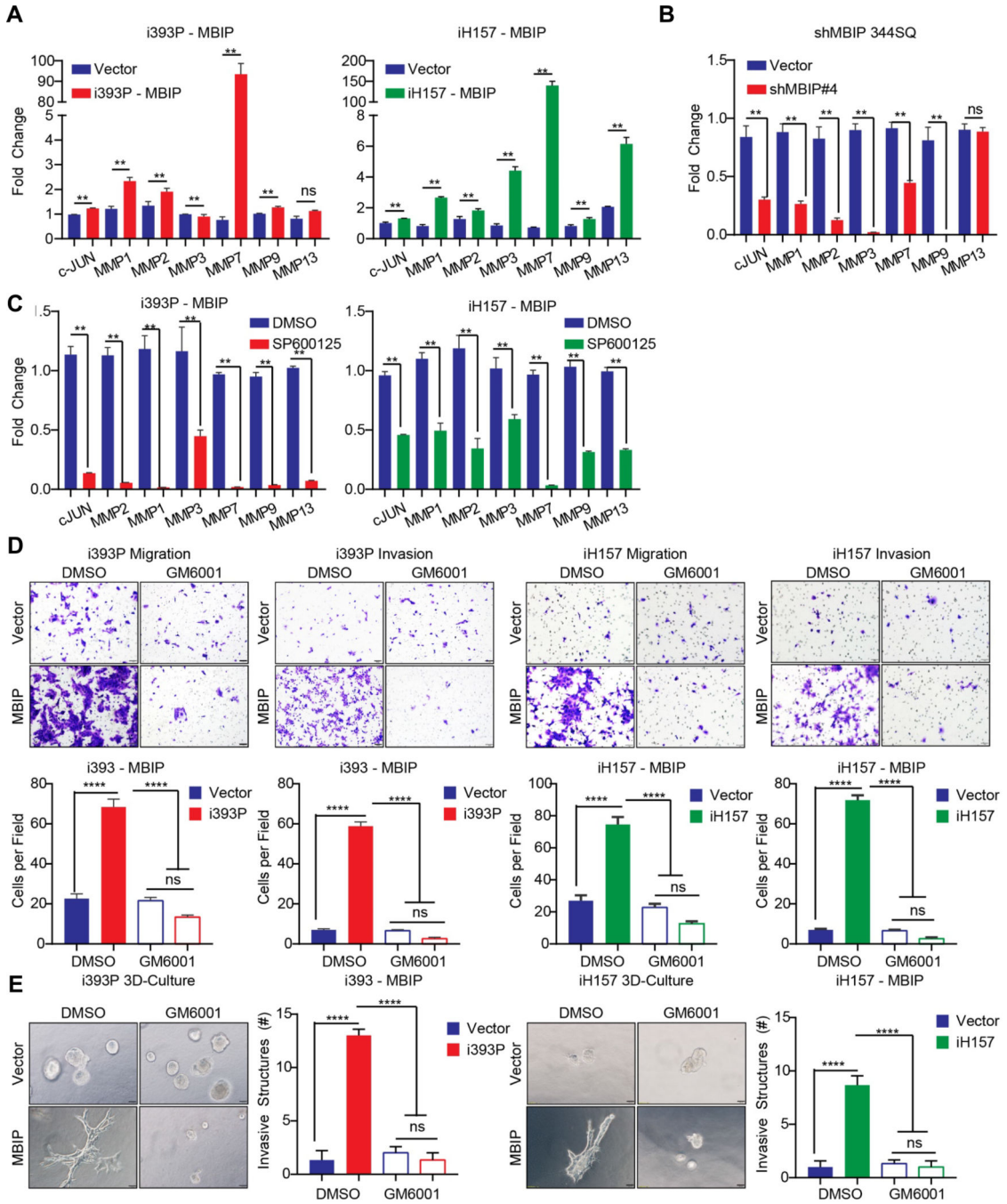
Figure 5. Inhibition of MMPs (GM6001) suppresses MBIP induced migratory and invasive potential.

qRT-PCR analysis for c-JUN and MMP family members performed using mRNA prepared from **(A)** i393P or iH157 cells with induced expression of MBIP or GFP as control and **(B)** 344SQ cells with stable knockdown of MBIP (shMBIP#4) or scramble control. All expression was normalized to the levels of L32. Note that different MMP levels are highly enriched as compared to the vector control and significantly lower in knockdown cells. **(C)** qPCR analysis for c-JUN and MMP family members performed using mRNA prepared from

i393P or iH157 cells with induced expression of MBIP or GFP as control, which are treated with a specific JNK inhibitor (SP600125) or DMSO as control. **(D)** Representative images of Transwell chamber assays performed for migration and invasion of i393P or iH157 cells, with induced expression of MBIP or GFP as control, which were treated with a pan-MMP inhibitor (GM6001) or DMSO as control. The number of cells migrated/invaded through the membrane/matrix were quantified as described in Materials and Methods **(E)** Representative images of 3D matrix (Matrigel+collagen) with invasive spheroids, formed by doxycycline-inducible MBIP-overexpressing i393P or iH157 cells, which were treated with a pan-MMP inhibitor (GM6001) or DMSO as control. Note the reduced number of invasive structures in MMP inhibited cells compared to the vector control. ****$P < 0.0001$ is based on the Student t test. All results are from three independent experiments. Error bars represent SD.
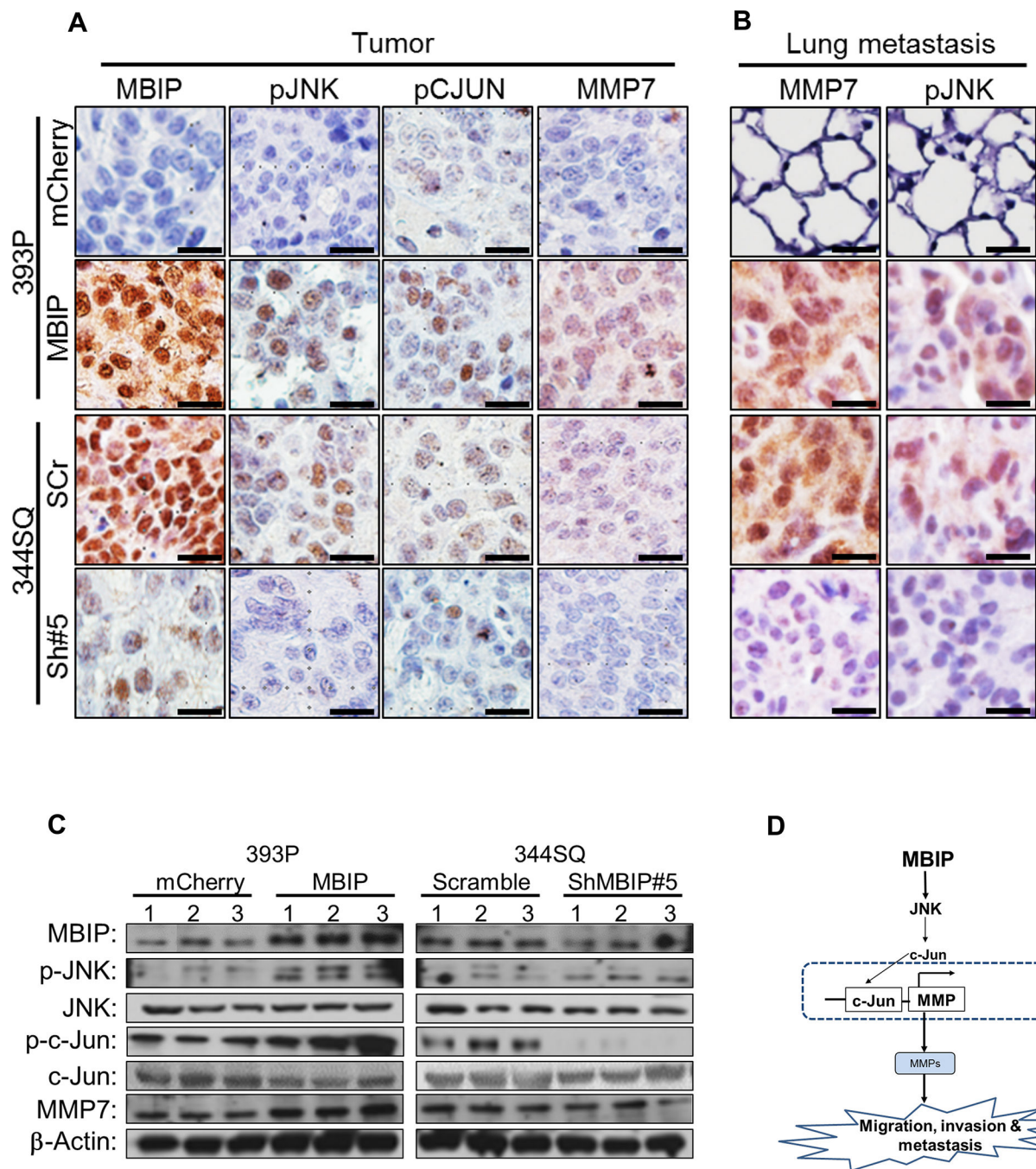
Figure 6. MBIP drives the JNK/c-JUN/MMP axis *in vivo*.
Representative IHC staining images from **(A)** Primary tumors or **(B)** metastatic lung lesions, from mice injected with MBIP-overexpressing (393-mCherry control and 393P-MBIP) and MBIP knockdown (344SQ-Scramble control and 344SQ-ShMBIP#5) cells, analyzed with antibodies against MBIP, p-JNK, p-c-Jun and MMP7. Scale bar = 50 μm. **(C)** Immunoblot analysis to determine expression levels of MBIP, p-JNK, total JNK, p-c-Jun, total c-Jun and MMP-7, in primary tumors formed by flank injection of MBIP-overexpressing (393-mCherry control and 393P-MBIP) and MBIP knockdown (344SQ-Scramble control and

344SQ-ShMBIP#5) cells as indicated. β-Actin was used as an internal loading control. **(D)** Schematic model: MBIP amplification leads to phosphorylation of JNK. Phosphorylated JNK actives c-JUN and AP-1 promoter which results into the transcription of MMPs, which is necessary for the increase in migration, invasion and metastasis.